33rd Annual International Conference of the IEEE EMBS
Boston, Massachusetts USA, August 30 - September 3, 2011

Optimal Multiresolution 3D Level-Set Method for Liver Segmentation incorporating Local Curvature Constraints

Daniel Jimenez-Carretero, Laura Fernandez-de-Manuel, Javier Pascau, Jose M. Tellado, Enrique Ramon, Manuel Desco, Andres Santos and Maria J. Ledesma-Carbayo

Abstract—**Advanced liver surgery requires a precise pre-operative planning, where liver segmentation and remnant liver volume are key elements to avoid post-operative liver failure. In that context, level-set algorithms have achieved better results than others, especially with altered liver parenchyma or in cases with previous surgery. In order to improve functional liver parenchyma volume measurements, in this work we propose two strategies to enhance previous level-set algorithms: an optimal multi-resolution strategy with fine details correction and adaptive curvature, as well as an additional semiautomatic step imposing local curvature constraints. Results show more accurate segmentations, especially in elongated structures, detecting internal lesions and avoiding leakages to close structures.**

I. Introduction

SURGICAL planning has been gaining importance over time in order to improve patient safety in complex surgical procedures, encouraged by improvements of medical imaging and new surgical devices. This is the case of advanced liver surgery [1], where certain modalities of liver transplant (e.g. living donor liver transplantation, split liver) and extreme hepatic resections require a precise description of liver anatomy (tumor size and location, vascular inflow and outflow, segmental divisions) as well as an estimation of minimum remnant liver volume [2] in order to avoid, for example, post-operative hepatic failure or "small-for-size" syndrome.

Preoperative CT or MR studies are, at the moment, the most important source of images that hepatic surgeons and radiologists employ for daily surgical planning. These studies are composed of hundreds of 2D slices. Commercial tools allow radiologists to manually segment 2D slices in axial views [3] with very simple algorithms. However, these manual segmentations are very time consuming. In this context, the development of automatic and semiautomatic algorithms for liver segmentation could speed up this task and remove human subjectivity.

Live wire algorithms [4] are the basis of semiautomatic liver volume extraction tools currently used in clinical practice. The first attempts to perform automatic liver segmentation were based on gray-level, trying to establish features related with liver density from statistical or histogram analysis or using mathematical morphology [5][6]. The most important problem of this kind of methods is that they do not take into account the high variability in CT images, the existence of different modality settings like contrast media, and the grey-level differences between healthy and pathological organs. Other works try to deal with these problems by using neural networks in order to learn gray-level features [7], but they usually need large training sets of images to capture the variability among patients. Deformable models, statistical shape models [8] and probabilistic atlases [9] try to learn anatomical features as shape, position and size, but they suffer from the same problems of neural network approaches, requiring too much computation time and failing when processing nonstandard liver shapes. Other different approaches use active contours algorithms. Snakes [10] and level-sets [11][12] are based on a speed function that controls the front propagation of a surface toward the liver boundary. Recently, most of new segmentation methods combine different techniques: statistical shape models, mathematical morphology and level-sets approaches. For an extensive review on novel liver segmentation methods, we refer the reader to [13].

II. Background on Level-Set Algorithm

Active contour models deal with automatic or semiautomatic delineation of objects in an image by evolving a curve guided by external constraint forces and influenced by image forces. This framework tries to minimize an energy function associated with these forces (external and internal, respectively). Traditionally, these models were based in edge detection by using gradient information. However, this approach fails when targets are not well-defined by gradients. In liver CT images this is an essential drawback due to the proximity between liver and other organs of similar intensity.

In order to deal with that problem Chan and Vese [14]

Manuscript received June 18, 2011. This study was partially supported by research projects PI09/91058, PI09/91065,ENTEPRASE PS-300000-2009-5, AMIT-CDTI, TEC2010-21619-C04 and PRECISION IPT-300000-2010-3, from Spain's Ministry of Science & Innovation, the project ARTEMIS Comunidad de Madrid, and with assistance from the European Regional Development Fund (FEDER).

Daniel Jimenez-Carretero, Laura Fernandez-de-Manuel, Andres Santos and Maria J. Ledesma-Carbayo are with the Group of Biomedical Image Technologies, ETSIT, Universidad Politécnica de Madrid, 28040 Spain and the CIBER-BBN, Spain. (e-mail: {daniel.jimenezc, lfernandez, andres, mledesma}@die.upm.es).

Javier Pascau and Manuel Desco are with "Medicina y Cirugía Experimental", Hospital General Universitario Gregorio Marañón, Madrid 28007, and Departamento de Bioingeniería e Ingeniería Aeroespacial, Universidad Carlos III de Madrid, Madrid 28911, Spain.

José M. Tellado is with the "Servicio de Cirugía General I", Hospital General Universitario Gregorio Marañón, Madrid 28007 Spain.

Enrique Ramón is with the "Servicio de Radiodiagnóstico", Hospital General Universitario Gregorio Marañón, Madrid 28007 Spain.

proposed an active contour model that takes into account intensity values inside and outside the curve, which can be formulated using level-set techniques as follows:

$$\frac{\phi_{i,j}^{n+1}-\phi_{i,j}^{n}}{\Delta t}=\delta_h(\phi_{i,j}^{n})\,[\mu\ div\left(\frac{\nabla\phi^n}{|\nabla\phi^n|}\right)-\gamma+ \quad (1)$$

$$\lambda_1(u_{0,i,j}-c_1(\phi^n))^2-\lambda_2(u_{0,i,j}-c_2(\phi^n))^2]$$

where ϕ represents the contour, u_0 is the image, c_1 and c_2 are the averages of u_0 inside and outside the contour respectively, $\mu\geq 0$, $\gamma\geq 0$, $\lambda_1,\lambda_2>0$ are fixed parameters, Δt and h are the time and space steps respectively and $div(\nabla\phi^n/|\nabla\phi^n|)$ introduces curvature constraints.

Nevertheless, this method works correctly only when the image is composed of two homogeneous regions with different textures. In CT abdominal images, liver region usually is homogeneous and well defined but the rest of the image includes several organs with different textures and intensities, compromising the correct behavior of the method.

In order to overcome this problem, Fernandez-de-Manuel et al. [15] presented a variation of this method, extended to 3D. They substitute the term that computes the intensity difference between a point and the average inside and outside the contour by a term that computes the absolute difference between these averages and include gradient information (controlled by the fixed parameter ρ) to achieve a more robust algorithm:

$$\frac{\phi_{i,j,k}^{n+1}-\phi_{i,j,k}^{n}}{\Delta t}=\delta_h(\phi_{i,j,k}^{n})\,[\mu\ div\left(\frac{\nabla\phi^n}{|\nabla\phi^n|}\right)-\gamma+ \quad (2)$$

$$\lambda_1\,|u_{0,i,j,k}-\rho\nabla u_{0,i,j,k}-c_1(\phi^n)|-\lambda_2\,|c_1(\phi^n)-c_2(\phi^n)|]$$

The algorithm starts with a seed point located inside the liver and grows a surface following a multi-resolution strategy in order to reduce processing time.

This approach achieved important improvements for liver segmentation results in CT abdominal images. However, these segmentations failed occasionally by including small areas belonging to proximal structures with similar intensity and texture, such as intercostal muscle and heart. In order to avoid the contour growing into these structures, Fernandez-de-Manuel et al. suggested establishing high restrictions in global curvature. As a result, elongated structures (distal part of liver left lobe, falciform ligament) were mis-segmented.

III. Proposed Method

In this paper, we contribute handling these difficulties with variations on (2). We propose an optimal multi-resolution strategy with fine details correction and an additional step imposing local curvature constraints.

A. Optimal Multi-Resolution Level-Set Segmentation.

Instead of using the same parameter values in all stages of the algorithm, we propose to change them depending on the resolution step by means of a multi-curvature, multi-growth strategy and a fine detail correction at the last multi-resolution level.

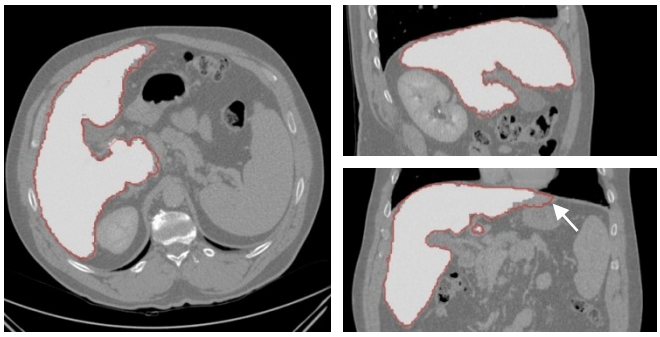

Fig. 1. Segmentation results obtained by the original level-set algorithm (white) and with a Multi-Growth restriction and Multi-Curvature strategy (red contour). Elongated zones are better segmented with the proposed strategy.

The basic idea is to apply a high global curvature restriction in first steps in order to limit the active contour expansion inside the liver and decreasing the probability of leaking. At low resolutions, structures are blurred and not well defined, making the separation of different organs a hard task. As we increase the resolution, structures and boundaries are better defined and we can relax the global curvature restriction (decreasing μ), allowing the contour to come closer to the desired segmentation.

Contrarily, we intensify the growth restriction along the multi-resolution scheme. At first, high values of λ_1 in (2) provide the contour with enough freedom to grow rapidly, and the gradual increment of the growth restriction in subsequent steps allows a better voxel classification inside or outside the level-set, emending mis-segmented structures.

The fusion of both strategies implies high growth of the contour in first resolution steps, limited by curvature constraints to avoid leakages, and low and controlled growth at the end with better detail detection and more accurate segmentation due to the relaxation of the global curvature restriction. The combination of both parameters improves segmentation results in elongated structures such as the distal part of liver left lobe (see Fig. 1). Thus, the fixed parameters λ_1, λ_2 and μ turn into functions depending on time (actually, resolution step): $\lambda_1(t),\lambda_2(t)$ and $\mu(t)$.

On the other hand, the level-set method implemented by Fernandez-de-Manuel et al. modifies the contour by checking voxels close to its boundary. This narrow band level-set approach is widely used because of the computation time improvement. However, this strategy combined with a multi-resolution scheme fails in the case of small structures at the inner part of the liver and far from its boundaries that are not big enough to be identified during contour growing in low resolution levels. In those cases, if the small non detected structures remain out of the narrow band, high resolution steps are not able to recover the wrong inclusion. This is the case of intraparenchymal small liver lesions and falciform ligaments, among others.

The fine details correction strategy tries to overcome this drawback by removing those voxels from the contour that have the highest intensity differences from the level-set mean intensity. Most of wrongly included structures have lower intensities than liver parenchyma, so we select a

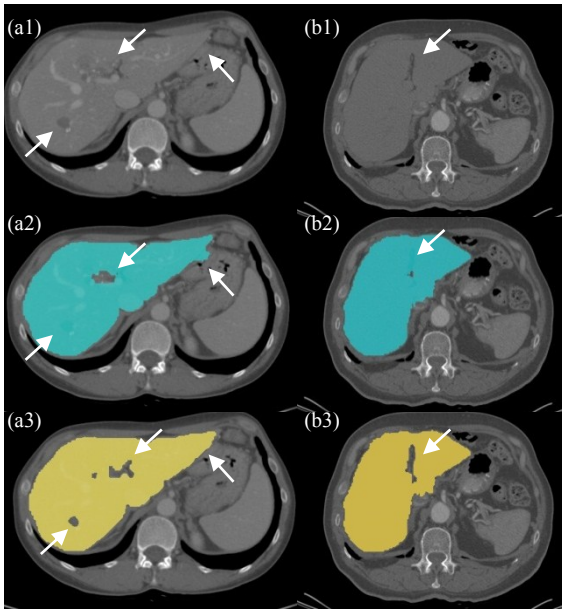

Fig. 2. Examples of livers slices with internal tumors and structures (a1, b1). Segmentations before (a2, b2) and after (a3, b3) introducing the fine details correction in the optimal multi-resolution strategy. The improvements in the detection of internal small lesions and falciform ligaments and the prevention of leakages are remarkable.

percentage of voxels with the lowest intensity, depending on the segmented volume, in order to remove them from the contour. After that, we erase as many voxels with the highest intensities as necessary to obtain the same average intensity we had at first, in order not to modify the level-set behavior.

This approach is used only before the last resolution step, so that, thanks to low global curvature constraint and high growth restriction, details can be detected and over-segmented structures can be identified. Furthermore, if some voxels are incorrectly removed, the level-set behavior will fix it in the last resolution step.

Results show internal tumors detection, a better liver lobes separation (due to detection of falciform ligaments and hepatic fissures) and decrease of leakages to proximal structures (see Fig. 2). In addition, in contrast enhanced CT images, some areas corresponding to large hepatic vessels as hepatic portal vein and upper suprahepatic veins are excluded from our results, which is the common practice by radiologists' manual segmentations of healthy parenchyma.

B. Local Curvature Constraints (LCC)

Liver segmentation is particularly challenging due to the variability in size and shape, especially in cases with big lesions or with prior surgery as hepatectomies. Using a priori knowledge could be inappropriate in these scenarios, so we propose to use LCC to restrict the contour growth in specific areas. Local mean curvature constraints were used before as priors obtained from statistical analysis of training sets [16], but this method could fail in the special cases mentioned above. So we let the user apply these local constraints by marking the problematic areas interactively. These marked voxels will be the center of a 3D Gaussian function that extends and distributes the curvature restriction in space.

$$G_{3D}(\vec{x},\sigma) = \frac{1}{(\sqrt{2\pi}\sigma)^3}\exp\left(\frac{-\|x\|^2}{2\sigma^2}\right) \quad (3)$$

where σ is the standard deviation and $\|\ .\ \|$ represents the Euclidean norm. Thus, curvature restriction will be different in each voxel x, following the equation:

$$C(\vec{x}) = \max(c_{global}, c_{\max}\cdot \max_j(G_{3D}(\vec{x}-\vec{x}_j^0,\sigma))) \quad (4)$$

where c_{max} is the maxima curvature, c_{global} the global curvature restriction in the image and x_j^0 are the points marked in problematic areas corresponding to the 3D Gaussian centers.

In order to check the performance and to obtain the best values for c_{max} and σ (which controls the size and magnitude of the 3D Gaussian function) in each resolution step, we created simulated images that contain areas with curvature changes (see Fig. 3). The best results were obtained with Gaussian size of 12.5x12.5x12.5 mm^3 and c_{max}=5. Thus, the function $\mu(t)$ becomes dependent on specific points marked, x_j^0, and the Gaussian parameters c_{max} and σ: $\mu(t, x_j^0, c_{max,}, \sigma)$.

IV. Data and Validation

The improvements on the liver segmentation tool have been validated on seven 3D abdominal CT images with variability in liver size, shape and position, different modality settings including or excluding contrast media and diverse pathological states (livers with primary or secondary tumors, livers ongoing lobar ipsolateral atrophy and contralateral hypertrophy after portal vein embolization, relapse tumors after liver lobectomies, and liver after hepatectomies undergoing chemotherapy). Study 3 was acquired on a Philips AV Expander spiral CT and the rest of cases were acquired on a Philips Brilliance 16 slice CT scanner. Pixel spacing varied from 0.69 to 0.84 mm in each slice, and the distance between slices was 5 mm in case 3; 3 mm in cases 6 and 7, and 1 mm in the rest of cases.

In all the cases, the gold standard was the segmentation of the healthy parenchyma made manually by radiologists on 2D slices in transversal views, excluding tumors, lesions and principal vessels such as cava and portal veins, in order to obtain more accurate estimations of functional liver volume.

The new algorithm uses 4 resolution steps with *#iterations=[200,150,100,70]* and parameters $h=1$, $1/\lambda_1=[5.5,5.5,7.5,x]$ with $x\in\{8,10,12.5\}$ depending on the image, $\lambda_2=[1,1,1,1]$ and $\mu=[1,1,0.75,0.5]$, fixed manually.

Five metrics were used to perform the validation: volumetric overlap error (VOE), relative volume difference (RVD) and average, root mean square and maximum symmetric

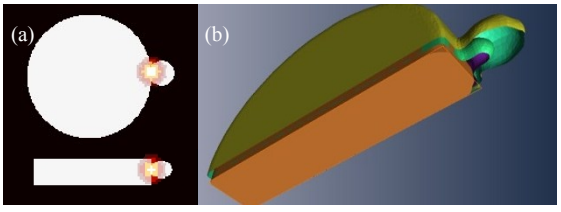

Fig. 3. (a) Simulated image with local curvature distribution obtained by marking a pixel as the center of the 3D Gaussian function. (b) 3D Reconstruction of the image (yellow) and segmentation results with LCC (orange) and without it (green).

TABLE I
SEGMENTATION RESULTS

Case	VOE [%]		RVD [%]		ASSD [mm.]		RMSD [mm.]		MSSD [mm.]		# LCC points	Time [min.]
	Original	New	Original	New	Original	New	Original	New	Original	New		
1	13.13	10.04	-9.02	-5.65	2.39	1.52	5.12	2.52	42.84	20.61	4	3.88
2	10.80	9.87	-5.76	-5.29	1.43	1.30	2.04	1.92	14.25	14.00	0	1.80
3	10.48	9.14	-6.38	-5.1	1.24	0.92	2.72	1.82	27.04	20.25	4	4.75
4	11.55	7.66	-4.46	-1.56	1.79	1.10	3.09	1.94	21.91	16.88	0	3.10
5	13.04	8.26	-9.41	-0.36	2.13	1.15	3.67	2.23	33.44	16.88	11	2.22
6	9.90	6.39	2.45	-3.22	1.42	0.67	3.59	1.37	30.43	13.45	5	2.73
7	8.12	4.40	1.55	1.57	1.12	0.52	3.22	1.69	33.11	23.54	10	3.00

surface distances (ASSD, RMSD, MSSD), described in [16].

V. RESULTS AND DISCUSSION

Table I shows the segmentation results, comparing the five different metrics between the original level-set algorithm [15] and the new one with the improvements described in this paper. Moreover, the number of points where the user established local curvature constraints and the computation times using an AMD Athlon II X4 630 processor 2.8 GHz and 6 GB of RAM have been included in the table. The results show absolute volume differences smaller than 6% in all the cases, with VOE between 4 and 10%, which evidence the improvements over previous results (decrease 3.04% in VOE on average). Avoiding overestimation of remnant liver volume is critical in surgical planning. For this reason, our algorithm tends to be conservative in almost all cases, obtaining negative volume differences caused by under-segmentation. Although these volume differences do not seem significant when the total non-tumoral parenchyma volume is considered, they have an important impact when the surgical strategy is defined and the quantification of the planned remnant liver is considered, where a 5 or 10% volume difference might overcome the threshold level for safety liver surgery.

The most relevant results are related with distance metrics. The better segmentation of elongated structures, internal tumors and the control of leakages performed high improvements in MSSD, achieving reductions of more than 15 mm. in some cases, which results in ASSD and RMSD improvements too. So, in all the cases, maximum distances correspond to points located in vessels, excluded from manual segmentations, but sometimes included in ours. Cases 1, 3 and 6 are specially challenging because contrast media was not used during the acquisition. In most cases, some local curvature constraints were added in principal vessels and areas between liver and close structures such as heart or stomach to avoid leakages toward these structures.

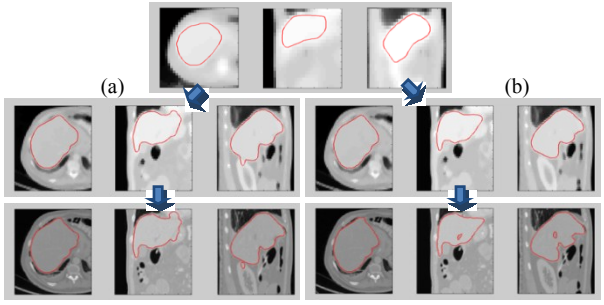

Fig. 4. Evolution of the Level-set algorithm comparing original approach (a) and the variation with proposed improvements (b), showing differences in the level-set behavior avoiding leakages in first steps and removing mis-segmented structures in the final results.

Fig, 4 shows the differences in the level-set evolution of the original and modified method, and illustrates a better behavior in unsettle areas wrongly segmented before. The proposed improvements have demonstrated good performance and results seem promising, but further studies are needed especially in vessel segmentation to achieve more accurate measures on remnant and non-tumoral liver volume.

REFERENCES

[1] M. Ryu and A. Cho, *The New Liver Anatomy: Portal Segmentation and the Drainage Vein*: Springer, 2009.

[2] C. B. Taner, *et al.*, "Donor safety and remnant liver volume in living donor liver transplantation," *Liver Transplantation,* vol. 14, pp. 1174-1179, 2008.

[3] A. Radtke, *et al.*, "Computer-assisted planning in living donor liver operation," *Zentralblatt Fur Chirurgie,* vol. 131, pp. 69-74, 2006.

[4] A. Schenk, *et al.*, "Local cost computation for efficient segmentation of 3D objects with live wire," *Medical Imaging 2001: Image Processing. Proc. SPIE*, Vol. 4322, pp. 1357-1364, 2001.

[5] H. Fujimoto, *et al.*, "Recognition of abdominal organs using 3D mathematical morphology," *Systems and Computers in Japan,* vol. 33, pp. 75-83, 2002.

[6] S. J. Lim, *et al.*, "Automatic segmentation of the liver in CT images using the watershed algorithm based on morphological filtering," *Medical Imaging 2004: Image Processing. Proc. SPIE*, Vol. 4322 p. 1658-1665, 2004.

[7] C. C. Lee, *et al.*, "Identifying multiple abdominal organs from CT image series using a multimodule contextual neural network and spatial fuzzy rules," *IEEE Transactions on Information Technology in Biomedicine,* vol. 7, pp. 208-217, 2003.

[8] H. Lamecker, *et al.*, "Segmentation of the liver using a 3d statistical shape model," ZIB-Report 04-09, 2004.

[9] X. Zhou, *et al.*, "Construction of a probabilistic atlas for automated liver segmentation in non-contrast torso CT images," in *CARS 2005: Computer Assisted Radiology and Surgery*, pp. 1169-1174, 2005.

[10] F. Liu, *et al.*, "Liver segmentation for CT images using GVF snake," *Medical Physics,* vol. 32, pp. 3699-3706, 2005.

[11] J. Lee, *et al.*, "Efficient liver segmentation exploiting level-set speed images with 2.5D shape propagation," *MICCAI 2007 Workshop: 3D Segmentation in the Clinic-A Grand Challenge*, pp. 189–196, 2007.

[12] L. Fernandez-de-Manuel, *et al.*, "Liver Segmentation and Volume Estimation from Preoperative CT Images in Hepatic Surgical Planning: Application of a Semiautomatic Method Based on 3D Level Sets," in *Theory and Applications of CT Imaging and Analysis*, N. Homma, (Ed.), InTech, pp. 79-94, 2011.

[13] T. Heimann, *et al.*, "Comparison and Evaluation of Methods for Liver Segmentation From CT Datasets," *IEEE Transactions on Medical Imaging,* vol. 28, pp. 1251-1265, 2009.

[14] T. F. Chan and L. A. Vese, "Active contours without edges," *IEEE Transactions on Image Processing,* vol. 10, pp. 266-277, 2001.

[15] L. Fernández-de-Manuel, *et al.*, "3D Liver Segmentation in Preoperative CT Images using a Level-Sets Active Surface Method," in *IEEE Engineering in Medicine and Biology Society*, pp. 3625-3628, 2009.

[16] T. Kohlberger, *et al.*, "Organ Segmentation with Level Sets Using Local Shape and Appearance Priors," in *MICCAI 2009*. vol. 5762, G.-Z. Yang, *et al.*, ed: Springer Berlin / Heidelberg, pp. 34-42, 2009.